Interactions between Surfactants and Cellulose Nanofibrils for Enhanced Oil Recovery

Trygve Dagsloth Jakobsen[1], Sébastien Simon[1], Ellinor Bævre Heggset[2], Kristin Syverud[1,2]*,

Kristofer Paso[1]

[1] Department of Chemical Engineering, NTNU Norwegian University of Science and Technology, 7491 Trondheim, Norway

[2] RISE PFI, Høgskoleringen 6b, 7491 Trondheim, Norway

*Corresponding author: kristin.syverud@rise-pfi.no, Tel.: +4795903740

Orcid:

Sébastien Simon: https://orcid.org/0000-0002-3101-4267

Ellinor Heggset: https://orcid.org/0000-0001-8876-8898

Kristin Syverud: https://orcid.org/0000-0003-2271-3637

Kristofer Paso: https://orcid.org/0000-0002-0502-9780

ABSTRACT

Chemical enhanced oil recovery (EOR) represents a series of potential solutions for extracting more oil from resources with already known locations and magnitudes. Unfortunately, many of the chemical additives in use today are not environmentally friendly. In the study a "greener" alternative for increasing viscosity of the injection water is investigated, namely cellulose

nanofibrils (CNF). The nanofibrils are combined in systems with anionic sulfonate surfactants, SDBS and AOT, in order to decrease interfacial tension (IFT) between oil and water. In combination, the increase of water viscosity and decrease of IFT should result in higher ultimate oil recovery than if only conventional water flooding was applied. Interactions between cellulose nanofibrils and the surfactants have been investigated through adsorption studies, rheology and IFT measurements. An observed synergy effect between CNF and surfactants upon viscosity of injection water, as well as with substantial decrease in IFT, leads the authors to the conclusion that an EOR system consisting of CNF and sulfonate surfactants has good potential for future applications.

1. INTRODUCTION

On the Norwegian continental shelf, over half of the original oil in place (OOIP) remains in the reservoir after production termination.[1] The ultimate oil recovery is even lower in most other oil producing nations. The potential for improving oil recovery worldwide is certainly immense. One method of improving oil recovery is by implementing chemical enhanced oil recovery (EOR) techniques, *i.e.* mixing chemical additives with the injection water, as either secondary or tertiary recovery method. The oil production can schematically be split into three phases. In the first one, the oil rises to the earth's surface driven by natural reservoir pressure. Once the underground pressure is no longer large enough to produce oil, then water or gas is injected to maintain pressure and oil production (secondary recovery). If water is injected, this phase is called water flooding. Finally, other methods can be implemented to extract even more oil, and increase the life span of the reservoir further and push additional oil towards the production well, so-called tertiary or

enhanced oil recovery. In recent years, it has become increasingly clear that the order of these measures could depend on the nature of the reservoir, and that injecting chemical additives could very well precede traditional water flooding. For offshore operations, seawater is typically used as the injection fluid. Three common mechanisms of chemical EOR are increasing sweep efficiency, reducing interfacial tension and altering rock wettability.[2]

One important reason why it is difficult to extract additional oil from reservoirs is that water is generally less viscous than the reservoir oil. This viscosity difference promotes flow of injected water during secondary recovery through zones of high permeability, leaving other zones largely unaffected by water flooding. The difference in mobility between oil and water results in a non-uniform displacement front, also known as viscous fingering. In order to reduce this effect, it is beneficial to artificially increase the injection water viscosity using additive substances.[2]

Injection water viscosity influences the capillary number, N_c, defined as the ratio of viscous forces to capillary forces, given in Eq. 1,

$$Nc = \frac{viscous\ forces}{capillary\ forces} = \frac{v\eta_w}{\gamma_{ow}cos\theta} \tag{1}$$

where v is brine velocity, η_w is brine viscosity, γ_{ow} is interfacial tension between oil and water, and θ is contact angle between rock and the wetting phase. Depending on the reservoir homogeneity, the capillary number may exhibit a large impact on ultimate oil recovery, as capillary forces trap oil within pores. The capillary number effect is quantified by utilizing capillary desaturation curves (CDC), which depict residual oil saturation as a function of capillary number. These curves are particularly dependent on the rock wettability condition.[3] In order to enhance oil recovery, the capillary number should optimally be elevated, which can be readily achieved either by increasing the injection water viscosity or by reducing the interfacial tension between oil and water.[4]

As a solution to the challenge of increasing the capillary number, polymer EOR has emerged as a subfield of chemical EOR. The most well-tested and used polymer to date is partially hydrolyzed polyacrylamide (HPAM), which is a water-soluble synthetic co-polymer consisting of adjustable fractions of polyacrylamide and polyacrylic acid.[5] HPAM exhibits acceptable toxicity and bioaccumulation values, but biodegradability is poor, which renders HPAM in the "red category" of offshore oil production chemicals, implying that it cannot be used without assurance that significant amounts will not be discharged to the environment.[1] Various biopolymers have been investigated as potentially environmentally friendly substitutes for HPAM, including xanthan gum and scleroglucan, which are both carbohydrates.[6] It was found that viscosifying properties of xanthan gum and schleroglucan in the semi-dilute regime are suitable for flooding, and they are both largely insensitive to electrolyte presence. However, reservoir conditions are typically detrimental to the use of these two polymers. Scleroglucan exhibits good temperature stability up to 105°C, while xanthan gum is adversely affected at 75°C. Bacterial degradation is an issue of concern with both biopolymers.[5]

Nanocellulose has in recent years been proposed as a competitive alternative to biopolymers in several applications, now also in EOR. Recently, Molnes *et al.*[7] investigated cellulose nanocrystals (CNC) as possible viscosifying agents for chemical EOR, and determined that the CNC particles have sufficient stability in salt, as well as satisfactory injectivity into porous sandstone.- A slight increase in incremental oil recovery was observed.[8] Aadland *et al.*[9] showed that salinity is the factor with greatest impact on injectability and retention in porous rock and sand similar to oil reservoirs. Heggset *et al.*[10] tested CNC as well as cellulose nanofibrils (CNF) for temperature stability, in the context of utilization at reservoir conditions. It was shown that the temperature

stability of TEMPO-CNF is superior to *e.g.* for xanthan. The improved thermal stability constitutes a major advantage, as reservoir temperatures are often over 90°C.[4]

Disintegration of wood pulp fibers into CNF was first described by Turbak *et al.*[11] and Herrick *et al.*[12] Initially, this process involved only high-pressure homogenization of wood pulp, but subsequently, various chemical pretreatments were shown to contribute to reduced energy consumption of production, and also leads to a more diversified range of surface chemistry and size distributions. One such pretreatment is TEMPO-mediated oxidation, utilizing 2,2,6,6-tetramethylpiperidine-1-oxyl radical (TEMPO) as a catalyst and NaOCl as oxidant, as first described by Saito and Isogai[13]. The TEMPO method yields a high density of carboxylic acid groups at the surface of the nanofibrils, which stabilizes the particles against aggregation in aqueous dispersion. Another production route is to use enzymes during pre-treatment, which selectively shears the β 1-4 bonds between monomers.[14] This enzymatic method typically yields fewer charges at the fibril surface.

CNF significantly increases apparent viscosity of aqueous media[15], carrying a much higher viscosifying potential than CNC due to the higher aspect ratio of CNF. Both CNF and CNC dispersions exhibit shear-thinning behavior, due to shear alignment of the particles.

Another mechanism for increasing the capillary number is to reduce interfacial tension between the oil and water phases. This is realized by injecting surfactants (surfactant flooding). Surfactants used in EOR are generally anionic in order to prevent absorption onto the rock phase.

Recently, Tichelkamp *et al.*[16] and Nourani *et al.*[17] extensively studied sodium dodecylbenzene sulfonate (SDBS) and sodium bis(2-ethylhexyl) sulfosuccinate (AOT) for usage in enhanced oil recovery, and have shown promising potential within this field. The comprehensive knowledge base surrounding these surfactants renders them a suitable choice for studying possible synergistic

effects between the surfactants and the cellulose nanofibrils and the low salinity water, and ultimately their combined performance efficiency for enhancing oil recovery.

Both AOT and SDBS give rise to very low interfacial tension in model oils and crude oils, and with some crude oils even ultralow interfacial tension, *i.e.* close to or lower than 1 μN/m. IFT values are strongly dependent on salinity and ionic composition of the solution. AOT and SDBS surfactants dissolved in salt-free water generally yield higher IFT towards oil in comparison to surfactants in low-salinity water, believed to be attributable to increased shielding by ions of electrostatic repulsion between surfactant head groups, which facilitates closer molecular packing at the interface. In addition, the presence of salt reduces the entropic penalty associated with the counter-ion layer at the interface, allowing increased adsorption. Low salinity (LS) water, or brine, is usually defined as less than 5000 ppm salt content, and LS reservoir flooding may in some cases enhance oil recovery in the absence of other additive chemicals.[18] In addition, replacing a portion of the sodium content with calcium may further reduce the IFT, especially in solution with SDBS, and more sporadically for AOT, depending on the specific oil.[19] IFT of SDBS behaves quite independently of solution pH at low salinity, both with and without Ca^{2+}, but salt-free surfactant solutions experience increased IFT at pH above 5 compared to pH~2. AOT solutions in LS and LS-Ca produce lower IFT values than SDBS for both model oils and crude oils.[19]

The use of chemicals in offshore oil production in the North-East Atlantic Ocean is regulated by the OSPAR convention, or the Convention for the protection of marine environment of the North-East Atlantic. For unrestricted use of a chemical, it must be accepted on the OSPAR PLONOR list[20] (considered to pose little or no risk to the environment), which requires it to adhere to established standards in the categories biodegradability, bioaccumulation and acute toxicity. All

chemicals on the PLONOR list are in the "Green category" according to OSPAR, but it does not contain any potential EOR surfactants.

AOT has demonstrated sufficient biodegradability[21] in primary degradation tests with a half-life degradation time of 7.5 days and ultimate biodegradability of over 60 %, which is sufficient to achieve the "yellow category". However, ultimate degradation values vary between studies, some exhibiting ultimate degradation lower than 60%, which only qualifies for the "Red category". The "Black category" contains the least acceptable chemicals, which are not to be used. Both "yellow" and "red" chemicals may potentially be applied if the risk of discharge to the environment is demonstrated to be low, or alternatively if the amount of discharged material is sufficiently low.

SDBS has been shown to be easily degradable in marine environments, characterized by a half-life less than 10 days.[1] Acute toxicity levels below 10 mg/L places SDBS in the "red" category.[22]

In the present work, we explore the potential of combined CNF and surfactants in EOR. The advantages of implementing such measures are many. CNF, an environmentally friendly material with improved thermal stability over other polysaccharides, and robust stability against shear degradation, increases brine viscosity and thereby also sweep efficiency. AOT and SDBS act upon capillary forces and mobilize oil in porous rock structures. However, possible interactions between these components must be understood prior to application planning. The effects of varying the brine viscosity and the interfacial tension between oil and water on capillary number has been previously studied on a fundamental level. In our model system, we have used TEMPO oxidized CNF, the surfactants SDBS and AOT, low salinity water of 1000 ppm NaCl, and dodecane as oil phase. Interactions were studied using various techniques including quartz crystal microbalance, rheology and interfacial tension measurements.

2. MATERIALS AND METHODS

Materials.

Cellulose nanofibrils were prepared by oxidation of cellulose with NaOCl, catalyzed by the presence of TEMPO and NaBr as previously described.[23] A fully bleached and never-dried softwood kraft pulp (donated by Södra Cell (Växjö, Sweden)) was used as source material. During oxidation, pH was adjusted and maintained close to 10 using NaOH (0.5 M), and afterwards neutralized to pH=7 using HCl (0.5 M). The pretreated cellulose pulp was filtered and washed repeatedly until a conductivity value of 5 μS/cm was attained. The pulp was grinded using a Masuko grinder prior to high-pressure homogenization (Rannie 15 type 12.56x homogenizer from APV, SPX Flow Technology, Silkeborg, DK), first 1 pass at 600 bar, and then 4 passes at 1000 bar.

Two commercial surfactants were purchased, SDBS (technical grade, Sigma-Aldrich) and AOT (96%, VWR International AS). The structure of both surfactants is presented in Figure 1. After dissolution in MQ-water, and/or mixing with other chemicals, samples were stirred for 10 min at 400-500 rpm. Critical micelle concentrations (CMC) in MQ-water were previously determined by Tichelkamp et al.[19] to be 1.69 mmol/L and 2.55 mmol/L for SDBS and AOT, respectively. Low salinity water was prepared at a concentration of 1000 ppm NaCl (99,5% Merck, Germany). An overview of samples and sample series used for the different analyses is shown in Table 1.
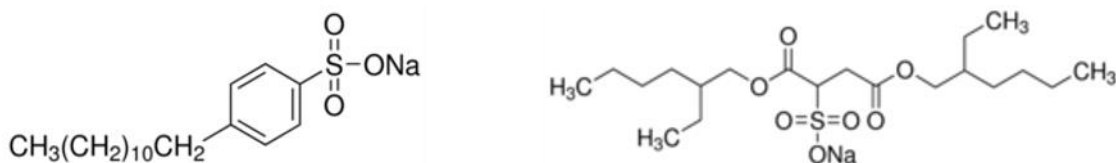

Figure 1: Chemical structure SDBS (left) and AOT (right) surfactants.

Table 1: Overview of samples and sample series investigated with each analytical method.

Method	CNF Manufacturer	CNF type	CNF conc. [wt/wt%]	Surfactant conc. [xCMC]	AOT conc. [g/L]	SDBS conc. [g/L]
AFM	RISE PFI	TEMPO oxized	0.02	0	0	0
QCM	Biolin Scientific	Enzymatically pretreated	N/A	0.1 - 10	0.11 - 11.34	0.059 - 5.89
Shear Viscosity	RISE PFI	TEMPO oxized	0.5	0.1 - 10	0.11 - 11.34	0.059 - 5.89
IFT	RISE PFI	TEMPO oxized	0.1	0.1 - 1.0	0.11 - 1.13	0.059 - 0.59

Methods.

Characterization of carbohydrate content

The composition of carbohydrates was determined according to the standard method NREL/TP-510-42618, using sulphuric acid hydrolysis. The composition of carbohydrate monomers produced during the hydrolysis was analysed using high-performance anion-exchange chromatography with pulsed amperometric detection (HPAEC-PAD; Dionex ICS-5000, (Thermo Fisher Scientific,Waltham, MA, USA) with a CarboPac PA1 column (Thermo Fisher Scientific, Waltham, MA, USA) and gradient elution using sodium hydroxide for elution.

Characterization of surface charge

Charge density measurements on pulp was performed via conductometric titration. After TEMPO-oxidation, water rinsing and neutralization, a small portion of pulp was extracted for charge density determination. The pulp was first protonized with 1% HCl, before washing away excess acid. The content of carboxyl and aldehyde groups was determined by conductometric titration using an automatic titrator (Metrohm 902 Titrado)[13]. The carboxylate content was determined from the titration curve. To determine the aldehyde content, oxidation of the aldehyde groups using $NaOCl_2$ was performed (Saito and Isogai, 2004)[13]. The aldehyde content was calculated from the difference in carboxylate content before and after oxidation.

Atomic Force Microscopy

Atomic force Microscopy (AFM) images were obtained with a Veeco diMultimode V instrument from Veeco Instruments Inc. (Santa Barbara, CA, USA). ScanAsyst mode was used along with operational mode quantitative nanomechanical mapping (QNM) with automated settings. Bruker AFM probes with silicon tips on nitride levers were used. The probes have a spring constant of 0.4 N/m. The image area was 2 x 2 μm. Nanoscope Analysis v1.40 was used to analyze the scans, and they were modified in ImageJ v1.50i. CNF samples were prepared according to Lahiji et al.[24] Mica discs of 10 mm width from Agar Scientific were cleaved and a drop of 0.02 wt% CNF suspension deposited. The surface was immediately rinsed with DI water, and compressed N_2 gas was used to dry the surface.

Adsorption studies

Adsorption measurements were performed using a Quartz Crystal microbalance (QCM-D) from Q-sense (Espoo, Finland). SiO_2 sensors coated with cellulose nanofibrils were purchased from Biolin Scientific. According to the manufacturer, the CNF was produced by enzymatic hydrolysis combined with mechanical shearing and high-pressure homogenization as described by Pääkkö et al.[14] (Material is called MFC by manufacturer.). Thickness of the cellulose layer was specified as ~6 nm with surface roughness 3-4 nm. Poly(ethylene) imine was used as adhesive between the cellulose layer and the silica. The temperature was 20 °C for all measurements. A stable baseline was first achieved for pure water for 5 minutes. Subsequently, surfactant solutions were introduced to the sensor, with a gradual increase in the surfactant concentration, beginning with the lowest concentration of surfactant, and gradually increasing. For each concentration, measurements were made during 5 minutes of pumping at 500 μL/min followed by 5 minutes of rest, whereupon

frequency and dissipation energy was acquired. After acquiring data at the highest concentration, the sensor was rinsed while recording data. Surfactant sample series in 1000 ppm NaCl were rinsed first with 1000 ppm NaCl, and then rinsed further with MQ-water. Surfactant sample series in MQ-water were rinsed directly with MQ-water. MQ-water rinse was performed for a duration of one hour for all samples. Each sensor was used a maximum of two times, and only for repetition of the same experiment. 2-3 parallels were acquired from each sample series. Mass adsorbed (Δm) was calculated from difference in frequency (Δf) using the relation described by Sauerbrey[25], given in eq. 2,

$$\Delta m = -\frac{\rho_q t_q}{f_0 n}\Delta f = -\frac{\rho_q v_q}{2 f_0^2 n}\Delta f = -\frac{C}{n}\Delta f \quad , \tag{2}$$

where ρ_q is the mass density of the crystal (=2648 kg/m^3), t_q is the crystal thickness (=0.3 mm); v_q is shear wave velocity in quartz (=3340 m/s), f_0 is the fundamental frequency of crystal (=5MHz) and n is the overtone number. The third overtone was selected for all results presented in this study.

Rheology

Rheology measurements were performed using a Physica MCR 301 from Anton Paar (Graz, Austria). A cone-and-plate geometry was used, with roughened surfaces on both contact surfaces. The cone is 40 mm wide with 2° angle, and during experiments, a gap size of 0.057 mm was employed. The analysis protocol began with 60 seconds of pre-shear rotation at 100 s^{-1} followed by 60 seconds of quiescent rest. Two cycles of increasing and decreasing shear rate ensued in a range of 0.1-1000 s^{-1}. The duration of each step in the program was 600 seconds, and the entire program had a duration of 42 minutes. All rheology analyses were performed at 20°C, and each analysis was performed at least twice.

Interfacial tension

Equilibrium interfacial tension (IFT) measurements were performed using a Sigma 70 Tensiometer (Espoo, Finland) with Platinum Du Noüy ring. Dodecane was used as a model oil. CNF, surfactant and salt were mixed in aqueous phase. Presented IFT values were all recorded after equilibrium state between oil and water phase had been reached. The equilibration time varied between samples, ranging from 2 hours to 15 hours, and was determined qualitatively as a point where the IFT value had not changed for at least one hour. All IFT experiments were conducted at 20 °C, and each experiment was performed at least twice.

3. RESULTS AND DISCUSSION

Characterization of the softwood pulp and the CNF quality

The carbohydrate composition of the softwood pulp was characterized as described in the experimental section, and the results are shown in Table 2.

Table 2: Carbohydrate composition of the softwood pulp.

Sample	Carbohydrate composition (weight%)				
	Glucan	Xylan	Mannan	Arabinan	Galactan
Softwood pulp	81.06	7.95	6.93	0.55	0.19

Charge density of the TEMPO-oxidized CNF was determined by conductometric titration to be 1128 μmol/g carboxylic acids and 178 μmol/g aldehyde groups.

AFM experiments were performed to visualize shape of CNF fibrils in absence of surfactants. AFM micrographs were acquired of CNF originally dispersed in MQ-water, but for this purpose dried on mica. Figure 2 shows a tight network of fibrils in several layers in the height dimension.

There is significant variation in diameters of fibrils, and aggregates of fibrils. Regarding the length of fibrils, no conclusion can be drawn based on this image, as the distance between particles is not sufficient to tell them apart. The image resembles other examples[10] of TEMPO-oxidized and homogenized CNF qualities from previous studies.
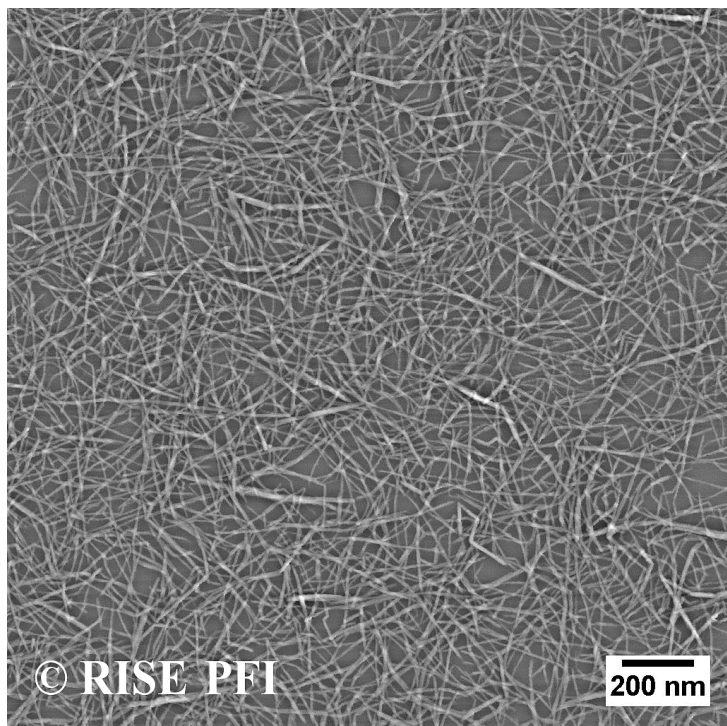

Figure 2: Atomic force microscopy image of cellulose nanofibrils dispersed on a mica disc.

Adsorption studies

Adsorption of surfactant onto CNF was measured directly by quartz crystal microbalance. An example of the experiments can be seen in Figure 3, where SDBS in MQ-water was introduced to the CNF-coated sensors. There is a linear relationship between decrease in frequency change (F) and increase in mass on the sensor. Dissipation change (D) increases with decreasing rigidity of the surface. Results of overtones n=3, n=5 and n=7 are presented. The lowest overtones probe

farthest from the sensor bottom, and overtone n=1 can even probe into the liquid phase, which makes it prone to noise.
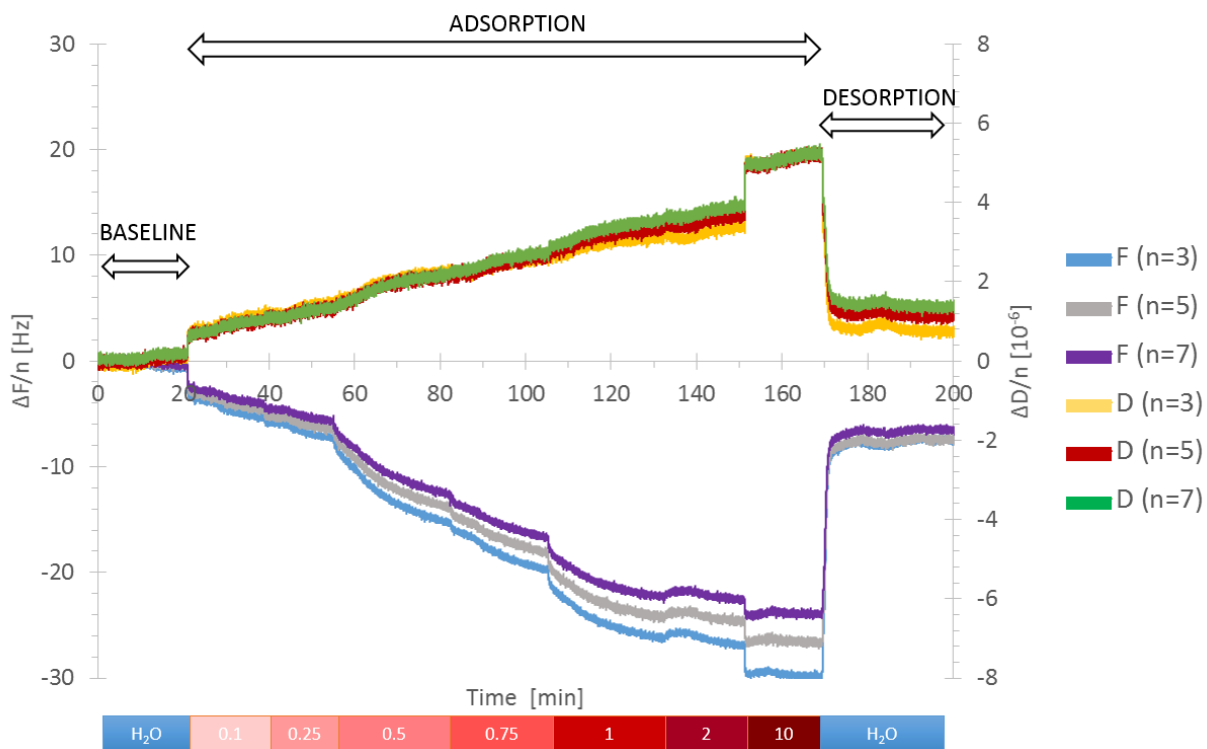

Figure 3: Frequency and dissipation changes for adsorption of SDBS in MQ-water onto CNF. Solutions were injected for 5 min of flow followed by 5 min of rest. Surfactant concentration was increased step-wise from 0.1xCMC to 10xCMC. Surfactant concentration is displayed at the bottom.

Figure 3 shows that SDBS adsorption in MQ-water is characterized by the spreading of frequency overtone and dissipation values above 10^{-6}. This means that the layer adsorbed onto cellulose is viscoelastic. In this article the adsorbed amount will be calculated from the Sauerbrey equation (n=3) owing to its simplicity. Even though the relation is valid only for even and rigid distribution of adsorbed mass on the surface, it provides a good measure of the adsorption process.

Adsorption of AOT onto CNF was measured directly by QCM, and is displayed in Figure 4. One sample series was diluted in MQ-water while the other was diluted at 1000 ppm (17 mM) NaCl. The sample series follow the same overall trend with gradual adsorption at low concentration, followed by a plateau at concentrations above CMC (2.55 mM). The CMC applied for surfactants in 1000 ppm was considered similar to the value in pure MQ-water in this article. With NaCl present, AOT adsorbs at slightly higher amounts than without NaCl, at low concentrations, but once concentration increases beyond 0.75xCMC, this difference is diminished. This difference may be attributed to screening of the electrical double layer on the surface of CNF particles, which arise from charged surface groups, as well as the reduced entropic penalty. Screening of the polar sulfonate head group on the AOT molecule is also affected and allows for reduced repulsion between surfactant and charged cellulose surface groups. Samples without NaCl adsorb even further from 2xCMC (~400 ng/cm^2) to the highest concentration of 10xCMC (~600 ng/cm^2). This effect cannot be identified in AOT samples with NaCl due to the large standard deviations at higher concentrations.
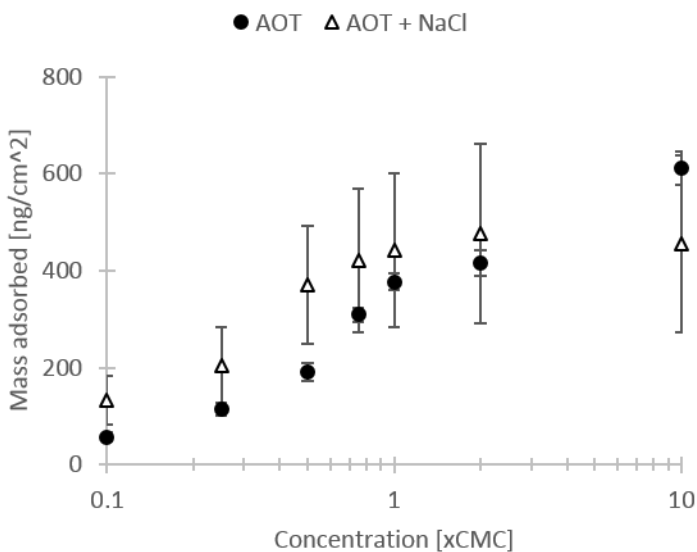
Figure 4: Adsorption of AOT surfactant in MQ-water and in 1000 ppm NaCl onto CNF coated silica surfaces as measured directly by QCM.

Adsorption of SDBS with and without NaCl was performed in the same manner as for AOT, and exhibited a much more pronounced salinity effect. The results are displayed in Figure 5, and it is clear that with salt present, adsorption of surfactant close to the plateau of maximum adsorption occurs already at the lowest surfactant concentration introduced. Both curves begin with a baseline at 0 ng/cm^2 in absence of surfactant. The SDBS sample series without NaCl, on the other hand, behaves much more like the AOT samples, with and without NaCl. An interesting development is that SDBS with and without NaCl end up at very much the same level of maximum adsorption, which is around 500 ng/cm^2. Above 1xCMC (1.69 mM), the two sample series exhibit similar behavior.
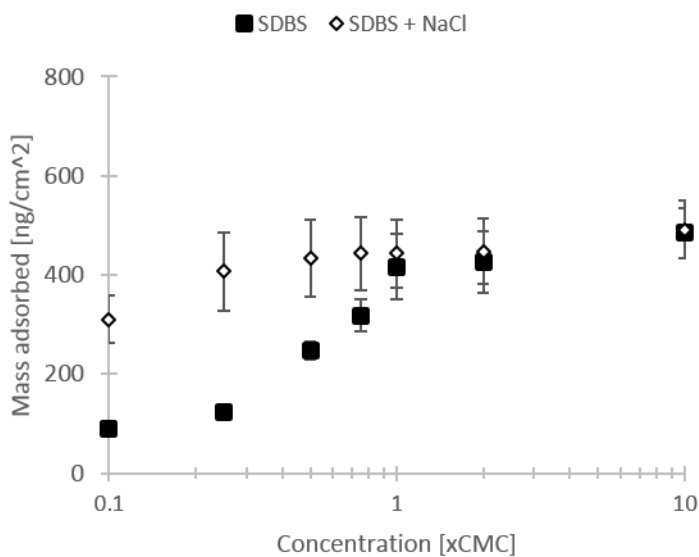

Figure 5: Adsorption of SDBS surfactant in MQ-water and in 1000 ppm NaCl onto CNF coated silica surfaces as measured directly by QCM.

These results are quite different from a study[26] on a similar surfactant, sodium dodecyl sulfate (SDS), which showed little adsorption under 2 mM, (~0.25xCMC) concentration but significant adsorption over this value, in the absence of salt. It was also reported that SDS aggregates assemble on the cellulose surface in the absence of salt, but with salt present only a thin layer (~15 Å) adsorbed. It must, however, be noted that the NaCl concentration was higher (100 mM) than in the current study (17 mM), and the manufacture and deposition of cellulose surface was not similar, as it consisted of deposition of a trimethylsilyl-cellulose layer, with subsequent cleaving of methyl groups.

Another work[27] studied adsorption of SDBS onto filter paper, showing similar values where maximum adsorption was attained at a concentration of 1.4 mM, which is just under 1xCMC. This study also showed a strong increase in surfactant adsorption with the presence of monovalent electrolyte (KCl) at various concentrations, and the maximum adsorbed amount increases significantly. This is different from the current results, showing that the maximum adsorbed amount is unaffected by NaCl in this range of concentration.

According to the manufacturer, the CNF layer on the sensor is ~6 nm thick, *i.e.* not more than a single layer of nanofibrils. This could indicate that large portions of the underlying silica surface will be exposed. In order to confirm that all adsorption occurs onto CNF and not onto silica, surfactants both with and without salt were also introduced to clean silica surface sensors. The experimental strategy used for CNF coated sensors was repeated for clean silica surfaces, and no mass change was observed whatsoever for the latter (results not shown).

After reaching stable levels of adsorbed mass for the highest concentration of surfactant (AOT: 25.5 mM; SDBS: 16.9 mM), the sensor surface was subsequently rinsed with water, and the mass change was observed. Sample series without NaCl were only rinsed with MQ-water, while sample

series containing NaCl were first rinsed with 1000 ppm NaCl until frequency stability was attained, and subsequently rinsed with MQ-water. The results are displayed in Figure 6. Sample series without NaCl show desorption between 80 and 90 % of maximum adsorbed mass when rinsed with MQ-water. Sample series with NaCl appear to desorb most adsorbed surfactant upon rinsing with low salinity water, and then desorb even more when rinsed with MQ-water. This proves that interactions responsible for adsorption of anionic surfactants onto nanocellulose are weak in nature.
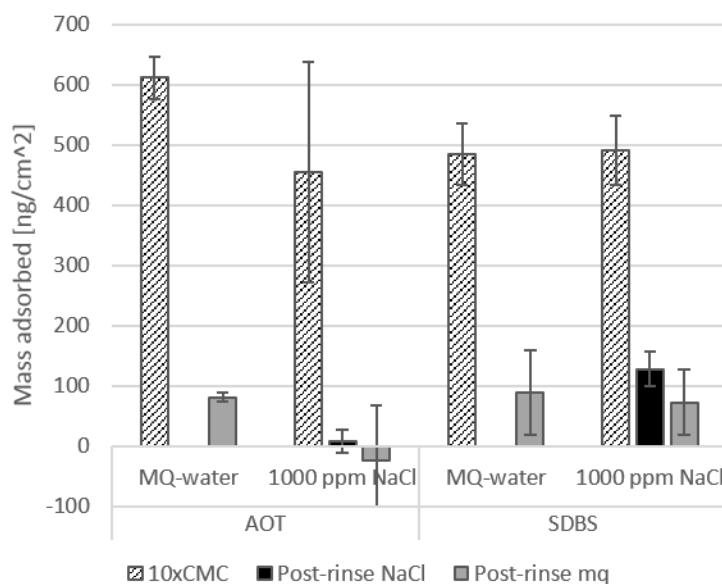

Figure 6: Surfactant desorption. Amount of adsorbed surfactant at the highest concentration and after rinse with MQ-water and 1000 ppm NaCl solution.

Tucker et al.[26] report high reversibility of adsorption of SDBS upon rinsing, in good agreement with the current results. Whether effective desorption is good for EOR applications or not is not a clear-cut case. The main mission of surfactants is to adsorb onto the oil-water interface, so it is useful that they are allowed to desorb from any other potential locations. At the same time, it is desirable to deploy surfactants far into to the interior of the reservoir in order to reduce IFT over a

volume as large as possible, and CNF particles may potentially act as carriers for the surfactants, in which cases a slow desorption may be preferable. In any case, SDBS adsorbs stronger to CNF in presence of NaCl than AOT does.

Rheology studies

Viscosity as function of shear rate was examined using a rheometer, on CNF dispersions in MQ-water, and with addition of AOT and SDBS surfactant and NaCl. Figure 7 shows results of only CNF in MQ-water, from the shear cycle used for all samples. After a pre-shear and subsequent resting step, shear rate begins at 0.1 s^{-1} and increases gradually to 1000 s^{-1} before receding back to the initial shear rate. Subsequently, the cycle is repeated once. This shows typical shear thinning behavior of CNF, which means that as shear rate increases, the viscosity decreases. This effect arises from alignment of the nanofibrils in the shear direction. The shear alignment effect is well-known, *e.g.* from Quennouz *et al.*[28], which also shows how viscosity at all shear rates increases with increasing CNF concentration.
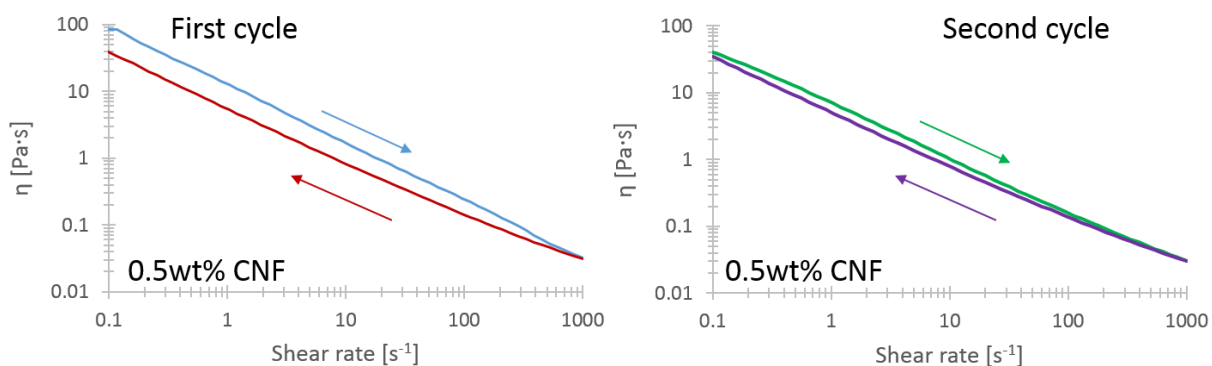
Figure 7: Example of typical shear rheology curves for CNF, showing viscosity as a function of shear rate. Concentration was 0.5 wt% CNF dispersed in MQ-water. All experiments followed the same shear program of two consecutive cycles of first increasing, then decreasing shear rate.

In the first cycle, the curves do not meet in the same value at shear rate 0.1 s^{-1}, and this is probably due to time dependence effects. The hysteresis between curves visible during the second cycle is due to another time dependence mechanism happening on a different time scale. The following results are from the first shear cycle, and values are generally for shear rate 1 s^{-1}.

Figure 8 shows the evolution of shear viscosity when SDBS and AOT surfactant is added to CNF in MQ-water. In terms of concentration in relation to the critical micelle concentration, the addition of the two surfactants behaves remarkably similar.
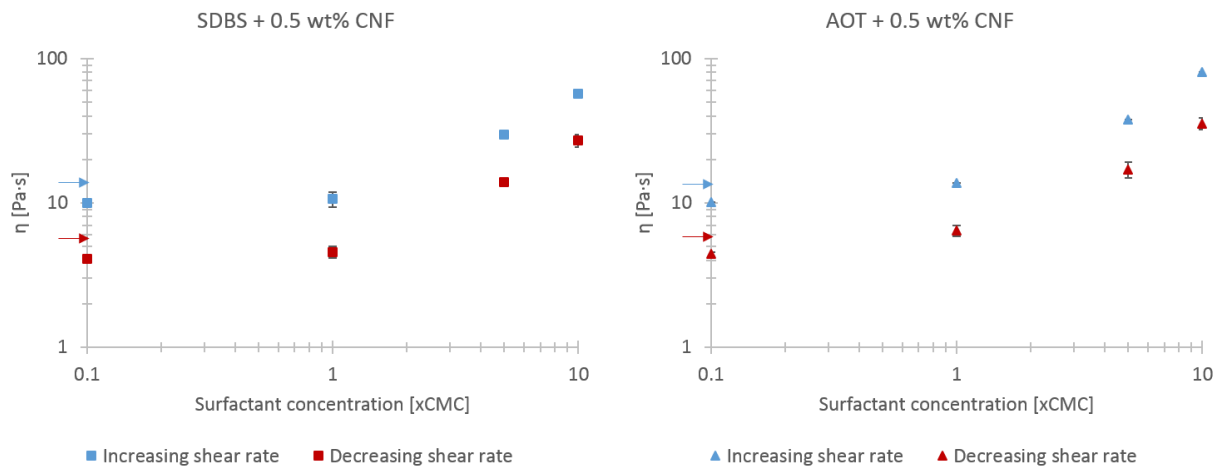

Figure 8: Shear viscosity of 0.5 wt% CNF with surfactant in MQ-water. Given values are from the first cycle of the rheology program, at shear rate $= 1 \text{ s}^{-1}$. Arrows indicate viscosity for CNF, without any surfactant present.

It is important to note that the two surfactants have quite different CMCs, 1.69 mmol/L for SDBS and 2.55 mmol/L for AOT, meaning that SDBS requires less concentration than AOT in terms of moles per volume to achieve the same effect on viscosity increase. In terms of mass per volume, SDBS requires roughly half the concentration relative to AOT. From pure CNF dispersion to addition of the lowest concentration of surfactant the viscosity decreases slightly, by 2-3 Pa·s at 1 s^{-1}, probably due to the increased ionic strength introduced by the surfactant, reducing electric double layer of the nanofibrils. Only a slight change is observed when increasing to 1xCMC, but upon further surfactant addition, the viscosity increases considerably. The QCM results show significant adsorption of both surfactants onto CNF below 1xCMC, and little further adsorption above CMC. These results do not correlate well as the observed change for adsorption and rheology occurs at two separate ranges of surfactant concentration. This may be attributable to the dissimilar nature of the TEMPO-oxidized CNF, which was analyzed with the rheometer, and the enzymatically pre-treated CNF used in adsorption studies. The former has quite high surface charge density, while the latter has generally few charges. Regarding the viscosity increase, Quennouz et al.[28] attribute gelation and viscosity increase of TEMPO-CNF in the presence of non-ionic and anionic surfactants to micelles bridging CNF particles. This overall picture fits well with the obtained results.

Figure 9 displays the shear-thinning index from shear viscosity flow curves. The power law relationship between shear rate and viscosity follows Eq. 3,

$$\eta = A\dot{\gamma}^{n-1} ,$$ (3)

where η is viscosity, $\dot{\gamma}$ is shear rate, A is consistency and n is the power law index.

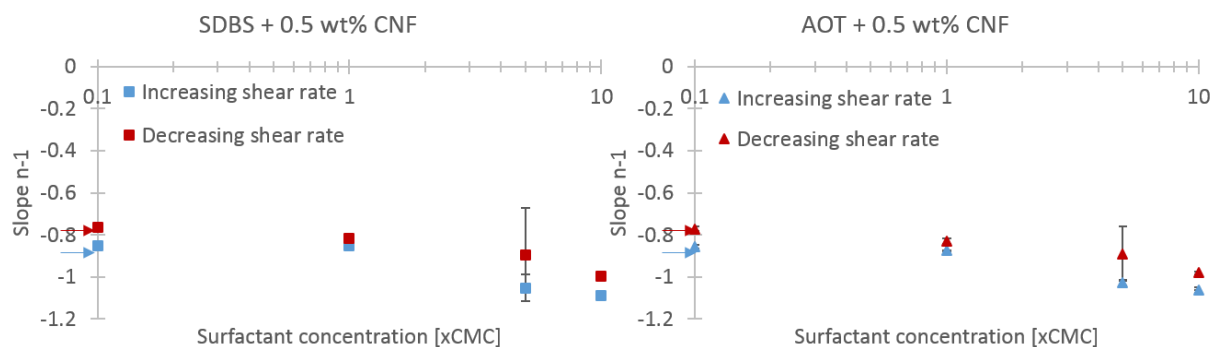Figure 9: The slope, n, of shear viscosity flow curves. Arrows indicate samples without surfactant.

The evolution of the slope means that the shear-thinning index is not constant. Surfactant concentrations higher than 1xCMC is thus shown to have an effect on the shear thinning behavior of CNF, indicating interactions between micelles and CNF. This variation in behavior can also be seen when plotting shear stress as function of shear rate: while in absence of surfactant, shear stress increases with shear rate, in presence of 10xCMC surfactant, shear stress is nearly constant for all the tested shear rates (results not shown).

Samples of pure surfactant in MQ-water were measured with the same method at concentrations of 5xCMC and 10xCMC. Both surfactant solutions showed same viscosity as pure water at all shear rates, which means that surfactants alone do not substantially contribute to viscosity without CNF present (results not shown). At higher concentrations of surfactant only, solution viscosity may increase due to self-assembly of large structures of surfactants, such as cylinders and aggregates of cylinders.[29]

The large difference in adsorption behavior observed by QCM for SDBS on CNF with and without NaCl may also be seen in the shear viscosity results, displayed in Figure 10. In the presence of salt, CNF dispersions exhibit substantially higher viscosity than in the absence of salt. This applies for samples not containing SDBS and samples containing concentrations up to

5xCMC. This indicates that the presence of salt (in low concentrations) contributes significantly to the viscosity increase, also without surfactant present. This effect is attributable to the decrease in extension of the electrical double layer when ionic strength is increased, and to some extent, the surfactant may contribute to the exact same effect, considering its ionic nature.
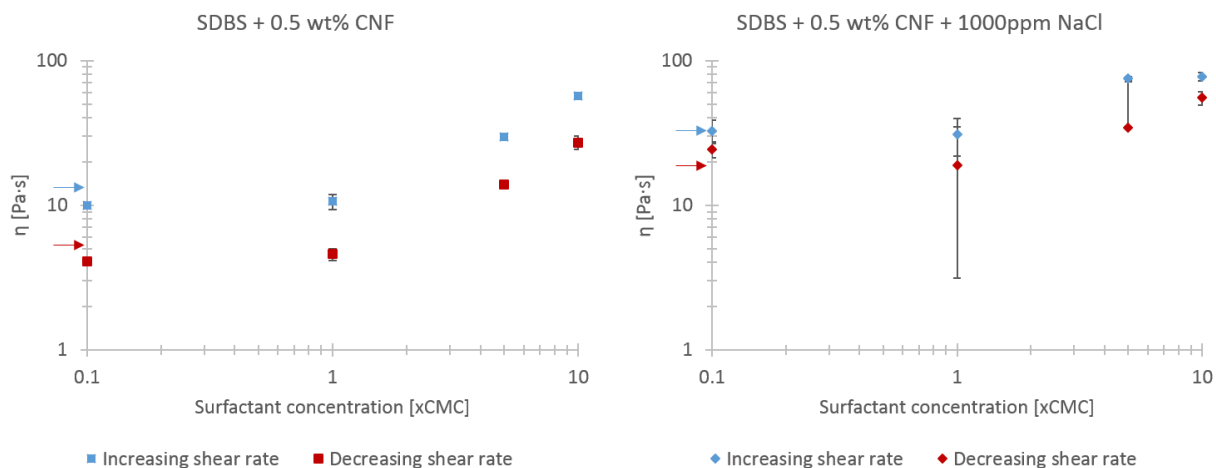

Figure 10: Shear viscosity of 0.5 wt% CNF with SDBS surfactant in 1000 ppm NaCl. Values are from the first cycle of the rheology program, at shear rate = 1 s^{-1}. Arrows indicate viscosity for CNF, without any surfactant present.

The maximum viscosity is independent of salt content within the low salinity range, but viscosity increase as a function of surfactant concentration increases with addition of 1000 ppm NaCl.

Interfacial tension

  As shown in previous studies, both SDBS[19] and AOT[30] are effective in reducing interfacial tension between water and alkanes, and between water and crude oil. CNF was combined with these surfactants to investigate the effect of CNF on IFT as well as possible synergy effects

between nanocellulose and surfactant, bearing in mind the adsorption of surfactant onto CNF particles. Figure 11 shows the decrease in IFT as surfactant is added, with and without the presence of CNF.

A small reduction in IFT can be seen between pure MQ-water and 0.1 wt% CNF in MQ-water. A reduction in the range between 2 and 5 mN/m is observed as result of addition of CNF, seemingly regardless of surfactant concentration.
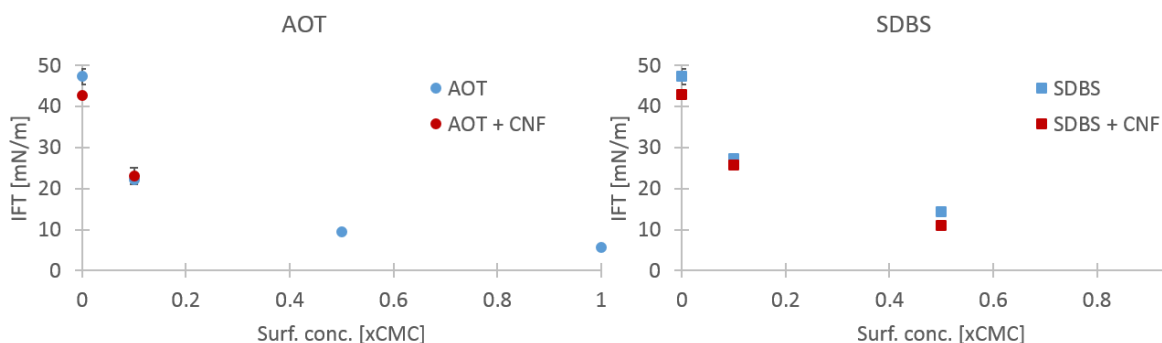

Figure 11: Interfacial tension of water/dodecane interface with addition of 0.1 wt% CNF and AOT surfactant (left) and SDBS surfactant

These results point to the conclusion that the IFT reducing effects of CNF and surfactant act in parallel, without appreciable synergies. CNF has an IFT reducing potential on its own, and AOT and SDBS surfactants reduce IFT without interference from CNF. This combination of IFT reduction, simultaneous to increase in viscosity, constitutes a major advantage for EOR flooding. QCM results exhibited efficient release of surfactant from the nanocellulose surface when subjected to more dilute brine. A potential strategy for flooding might be to let CNF act as a carrier for surfactants, releasing molecules far into the distance of the reservoir, while maintaining an acceptable level of injection water viscosity. The effect could be that surfactants are transported

farther than they would without nanoparticles, facilitating mobilization of oil droplets over a larger volume of the reservoir.

Capillary number

Capillary number has been calculated using Eq. 1 for different combinations of parameters, and is displayed in Table 3. Contact angles between rock and wetting phase used for silica and calcite was 5.5° and 22°, respectively[31].

Table 3: Relative values of capillary number divided by brine velocity (N_C/v [s/m]).

Shear rate	Pure water		AOT		SDBS		SDBS + NaCl	
	Silica	Calcite	Silica	Calcite	Silica	Calcite	Silica	Calcite
1 s^{-1}	$2.1 \cdot 10^{-2}$	$2.3 \cdot 10^{-2}$	$1.4 \cdot 10^{4}$	$1.5 \cdot 10^{4}$	$8.2 \cdot 10^{3}$	$8.8 \cdot 10^{3}$	$1.2 \cdot 10^{4}$	$1.2 \cdot 10^{4}$
10 s^{-1}	$2.1 \cdot 10^{-2}$	$2.3 \cdot 10^{-2}$	$7.1 \cdot 10^{2}$	$7.6 \cdot 10^{2}$	$3.7 \cdot 10^{2}$	$4.0 \cdot 10^{2}$	$7.1 \cdot 10^{2}$	$7.7 \cdot 10^{2}$

The table shows that for low shear values, the capillary number can improve by six orders of magnitude and by four orders of magnitude for medium shear rate. This increase is mostly due to the large viscosity increase caused by addition of CNF. It should be mentioned that far lower IFT values than the current results have been obtained for AOT[30] and SDBS[19] in previous scientific work. IFT values in the current study was performed using a tensiometer unable to measure values under ~1 mN/m, which is the case with large surfactant concentrations. Optimization of IFT reduction and viscosity increase could further increase the capillary number by more than one order of magnitude. Such a significant increase in capillary number is theoretically well within the margin for a large improvement in incremental oil recovery.[3]

4. CONCLUSIONS

Cellulose nanofibrils have been proposed as environmentally friendly alternatives to synthetic polymers as viscosity enhancers in chemical enhanced oil recovery. Relevant physical properties of CNF have been investigated in combination with introduction of model surfactants, AOT and SDBS, which have characteristics suitable for EOR. Adsorption of surfactant onto CNF was measured and the results showed that AOT adsorbed similarly with no salt present and with 1000 ppm NaCl present. A different result was observed for SDBS, which adsorbed much more effectively with NaCl present, but the maximum adsorbed amount above CMC was the same as in pure water. SDBS and AOT adsorbed in very similar amounts as function of concentration in relation to the CMC. Interfacial tension measurements showed that CNF alone reduces IFT slightly between oil and water, regardless of surfactant concentration. As previously demonstrated, SDBS and AOT are potent IFT reduction agents. Both SDBS and AOT surfactants have a synergistic effect on viscosity of CNF dispersions, contributing substantially to viscosity increase. This effect on viscosity is similar in pure water and in low-salinity water. Micelle bridging between fibrils is believed to be the cause of the viscosity increase. There are few differences between SDBS and AOT with respect to the physical properties investigated in the current study, when presented as function of the critical micelle concentration. SDBS has a CMC well below that of AOT, and as function of mass per volume, one may attain similar results with roughly half the amount of SDBS as the required amount of AOT. The potential difference in capillary number upon addition of EOR systems consisting of CNF and AOT and SDBS surfactants is at least four orders of magnitude.

(1)   FORCE Assessment of environmental impact from EOR chemicals for the Norwegian Continental Shelf. **2011**.

(2)   Terry, R. E. Enhanced Oil Recovery. In *Encyclopedia of Physical Science and Technology*, 3rd ed.; Meyers, R. A., Ed. Academic Press, **2001**; Vol. 18, pp 503-518.

(3)   Guo, H.; Dou, M.; Hanqing, W.; Wang, F.; Yuanyuan, G.; Yu, Z.; Yansheng, W.; Li, Y. Review of Capillary Number in Chemical Enhanced Oil Recovery. In *SPE Kuwait Oil and Gas Show and Conference*, Society of Petroleum Engineers: Mishref, Kuwait, **2015**.

(4)   Sheng, J. J. Status of surfactant EOR technology. *Petroleum* **2015,** *1* (2), 97-105.

(5)   Olajire, A. A. Review of ASP EOR (alkaline surfactant polymer enhanced oil recovery) technology in the petroleum industry: Prospects and challenges. *Energy* **2014,** *77*, 963-982.

(6)   Sveistrup, M.; van Mastrigt, F.; Norrman, J.; Picchioni, F.; Paso, K. Viability of Biopolymers for Enhanced Oil Recovery. *Journal of Dispersion Science and Technology* **2015**, 1160-1169.

(7)   Molnes, S. N.; Torrijos, I. P.; Strand, S.; Paso, K. G.; Syverud, K. Sandstone injectivity and salt stability of cellulose nanocrystals (CNC) dispersions—Premises for use of CNC in enhanced oil recovery. *Industrial Crops and Products* **2016,** *93*, 152-160.

(8)   Molnes, S. N.; Mamonov, A.; Paso, K. G.; Strand, S.; Syverud, K. Investigation of a new application for cellulose nanocrystals: a study of the enhanced oil recovery potential by use of a green additive. *Cellulose* **2018**.

(9)   Aadland, R.; Dziuba, C.; Heggset, E.; Syverud, K.; Torsæter, O.; Holt, T.; Gates, I.; Bryant, S. Identification of Nanocellulose Retention Characteristics in Porous Media. *Nanomaterials* **2018,** *8* (7), 547.

(10)   Heggset, E. B.; Chinga-Carrasco, G.; Syverud, K. Temperature stability of nanocellulose dispersions. *Carbohydrate Polymers* **2017,** *157*, 114-121.

(11)   Turbak, A. F.; Snyder, F. W.; Sandberg, K. R. Microfibrillated cellulose, a new cellulose product: Properties, uses and commercial potential. *Journal of Applied Polymer Science* **1983,** *37*, 815-827.

(12)   Herrick, F. W.; Casebier, R. L.; Hamilton, J. K.; Sandberg, K. R. Microfibrillated cellulose: morphology and accessibility. *Journal of Applied Polymer Science, Applied Polymer Symposium* **1983,** *37*, 797-813.

(13)   Saito, T.; Isogai, A. TEMPO-Mediated Oxidation of Native Cellulose. The Effect of Oxidation Conditions on Chemical and Crystal Structures of the Water-Insoluble Fractions. *Biomacromolecules* **2004,** *5* (5), 1983-1989.

(14)   Pääkkö, M.; Ankerfors, M.; Kosonen, H.; Nykänen, A.; Ahola, S.; Österberg, M.; Ruokolainen, J.; Laine, J.; Larsson, P. T.; Ikkala, O.; Lindström, T. Enzymatic Hydrolysis Combined with Mechanical Shearing and High-Pressure Homogenization for Nanoscale Cellulose Fibrils and Strong Gels. *Biomacromolecules* **2007,** *8* (6), 1934-1941.

(15)   Jowkarderis, L.; van de Ven, T. M. Intrinsic viscosity of aqueous suspensions of cellulose nanofibrils. *Cellulose* **2014,** *21* (4), 2511-2517.

(16)   Tichelkamp, T.; Hosseinzade Khanamiri, H.; Nourani, M.; Stensen, J. Å.; Torsæter, O.; Øye, G. EOR Potential of Mixed Alkylbenzene Sulfonate Surfactant at Low Salinity, and the Effect of Calcium on "Optimal Ionic Strength". *Energy & Fuels* **2016,** *30*, 2919-2924.

(17)   Nourani, M.; Tichelkamp, T.; Gaweł, B.; Øye, G. Method for Determining the Amount of Crude Oil Desorbed from Silica and Aluminosilica Surfaces upon Exposure to Combined Low-Salinity Water and Surfactant Solutions. *Energy & Fuels* **2014,** *28* (3), 1884-1889.

(18)   McGuire, P. L.; Chatham, J. R.; Paskvan, F. K.; Sommer, D. M.; Carini, F. H. Low Salinity Oil Recovery: An Exciting New EOR Opportunity for Alaska's North Slope. In *SPE Western Regional Meeting*, Society of Petroleum Engineers: Irvine, California, **2005**.

(19)   Tichelkamp, T.; Vu, Y.; Nourani, M.; Øye, G. Interfacial Tension between Low Salinity Solutions of Sulfonate Surfactants and Crude and Model Oils. *Energy & Fuels* **2014,** *28* (4), 2408-2414.

(20)   OSPAR List of Substances Used and Discharged Offshore which Are Considered to Pose Little or No Risk to the Environment (PLONOR) – Update 2018. https://www.ospar.org/work-areas/oic/chemicals (accessed 2018.08.14).

(21)   Steber, J.; Berger, H. Biodegradability of anionic surfactants. In *Biodegradability of Surfactants*, Karsa, D. R.; Porter, M. R., Eds. Springer Netherlands: Dordrecht, **1995**; pp 134-182.

(22)   Ying, G.-G. Fate, behavior and effects of surfactants and their degradation products in the environment. *Environment International* **2006,** *32* (3), 417-431.

(23)   Saito, T.; Nishiyama, Y.; Putaux, J.-L.; Vignon, M.; Isogai, A. Homogeneous Suspensions of Individualized Microfibrils from TEMPO-Catalyzed Oxidation of Native Cellulose. *Biomacromolecules* **2006,** *7* (6), 1687-1691.

(24)   Lahiji, R. R.; Xu, X.; Reifenberger, R.; Raman, A.; Rudie, A.; Moon, R. J. Atomic Force Microscopy Characterization of Cellulose Nanocrystals. *Langmuir* **2010,** *26* (6), 4480-4488.

(25)   Sauerbrey, G. Verwendung von Schwingquarzen zur Wägung dünner Schichten und zur Mikrowägung. *Zeitschrift für Physik* **1959,** *155* (2), 206-222.

(26)   Tucker, I. M.; Petkov, J. T.; Penfold, J.; Thomas, R. K. Interaction of the Anionic Surfactant SDS with a Cellulose Thin Film and the Role of Electrolyte and Poyelectrolyte. 2 Hydrophilic Cellulose. *Langmuir* **2012,** *28* (27), 10223-10229.

(27)   Paria, S.; Manohar, C.; Khilar, K. C. Adsorption of anionic and non-ionic surfactants on a cellulosic surface. *Colloids and Surfaces A: Physicochemical and Engineering Aspects* **2005,** *252* (2), 221-229.

(28)   Quennouz, N.; Hashmi, S. M.; Choi, H. S.; Kim, J. W.; Osuji, C. O. Rheology of cellulose nanofibrils in the presence of surfactants. *Soft matter* **2015,** *12*, 157-164.

(29)   Holmberg, K., Jönsson, B., Kronberg, B., Lindman, B. *Surfactants and Polymers in Aqueous Solution*. 2nd ed.; John Wiley & Sons, Ltd: The Atrium, Southern Gate, Chichester, West Sussex PO19 8SQ, England, **2006**.

(30)   Tichelkamp, T.; Teigen, E.; Nourani, M.; Øye, G. Systematic study of the effect of electrolyte composition on interfacial tensions between surfactant solutions and crude oils. *Chemical Engineering Science* **2015,** *132*, 244-249.

(31)   Pradilla, D.; Subramanian, S.; Simon, S.; Sjöblom, J.; Beurroies, I.; Denoyel, R. Microcalorimetry Study of the Adsorption of Asphaltenes and Asphaltene Model Compounds at the Liquid–Solid Surface. *Langmuir* **2016,** *32* (29), 7294-7305.

For table of contents only